Science Signaling
AAAS

www.sciencesignaling.org/cgi/content/full/4/194/ra68/DC1

Supplementary Materials for

Phosphorylation of Mad Controls Competition Between Wingless and BMP Signaling

Edward Eivers, Hadrien Demagny, Renee H. Choi, Edward M. De Robertis*

*To whom correspondence should be addressed. E-mail: ederobertis@mednet.ucla.edu

Published 11 October 2011, *Sci. Signal.* **4**, ra68 (2011)
DOI: 10.1126/scisignal.2002034

The PDF file includes:

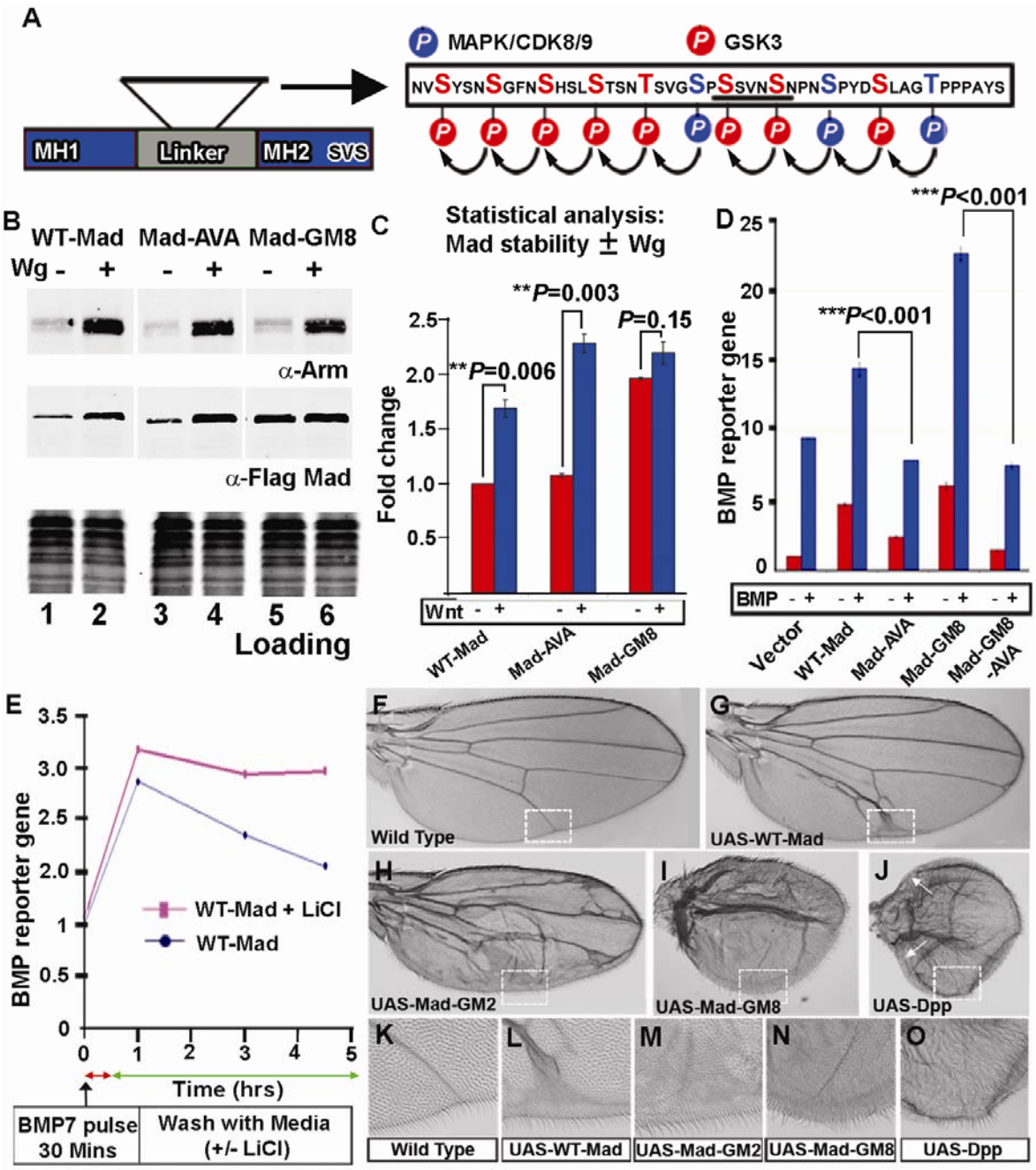

figure S1. Increased BMP signals generated by a stabilized Mad protein. In the Mad GSK3 mutant 8 (Mad-GM8), the eight putative GSK3 sites were rendered resistant to phosphorylation by mutating Ser or Thr to Ala. **(A)** Schematic diagram highlighting the putative phosphorylation sites in the linker region of Mad. Three potential MAPK or CDK8 and CDK9 priming phosphorylations (Ser-Pro) are highlighted in blue. The eight putative GSK3 phosphorylations in

Mad are indicated in red. **(B)** Flag-tagged WT-Mad is significantly stabilized in cells treated with Wg-conditioned medium compared to cells treated with conditioned medium from cells not transfected with Wg (compare lanes 1 and 2). Mad-AVA, which is resistant to C-terminal phosphorylation, is also stabilized by Wg protein (lanes 3 and 4). Mutation of all eight GSK3 phosphorylation sites in the linker region of Mad (Mad-GM8) causes stabilization of the protein even in the absence of Wg conditioned medium (lanes 5 and 6). Armadillo, a protein that is stabilized by Wg, is used to demonstrate activation of Wg signaling. Equal loading is shown in the coomassie blue image (n = 4 blots). **(C)** Analysis by Mann-Whitney-Wilcoxon test of the stability of Mad from immunoblots quantified using the LI-COR Odyssey system. **(D)** BMP reporter gene (BRE-luciferase) activity was increased when GSK3 phosphorylation sites in Mad (Mad-GM8) were mutated. BMP stimulation did not increase BMP reporter activity above basal values in cells expressing Mad-GM8-AVA ($P < 0.001$, brackets; 2-way ANOVA with Tukey's post-test). These experiments demonstrate that Mad-GM8 enhances the effects of BMP signaling by increasing the duration of the BMP signal, but only when C-terminal phosphorylation is possible (n = 3 experiments). **(E)** 30-minute incubation with BMP7 was performed at the beginning of this assay. The duration of the BMP signal was prolonged by inhibiting GSK3 phosphorylation with LiCl, a treatment that mimics the Wg signal. **(F)** Wild-type adult wing, showing normal venation. **(G)** A moderate increase in vein tissue in adult wings was seen when WT-Mad was driven with MS1096-Gal4 (n = 23). **(H)** In adult wings with a form of Mad bearing two mutated GSK3 phosphorylation sites (Mad GSK3 mutant 2; Mad-GM2), vein formation was increased (n = 34) (*1*). **(I)** Overexpression of Mad-GM8 protein resulted in increased venation (n = 45, all specimens showed similar phenotypes). The shape of the adult wing also adopted a more circular shape compared to wild-type wings. **(J)** Dpp overexpression generated vein and wing shape phenotypes similar to those of Mad-GM8 overexpression (n =

20). Dpp overexpression causes loss of margin bristles (white arrows), a typical Wg loss-of-function phenotype (*2*). **(K)** High magnification of boxed region in (B) showing the distal portion of vein 5. Note that vein cells were smaller than intervein cells. **(L)** High magnification of longitudinal vein 5 showing that WT-Mad overexpression mildly increased distal venation forming a delta structure towards the margin. **(M)** High magnification of Mad-GM2 overexpressing wings showing transformation of intervein tissue into vein tissue. **(N)** High magnification of Mad-GM8 overexpressing wings showing that intervein tissue displayed the smaller cell phenotype characteristic of vein tissue. **(O)** Dpp overexpression, like Mad-GM8 overexpression, transforms intervein tissue into vein tissue.

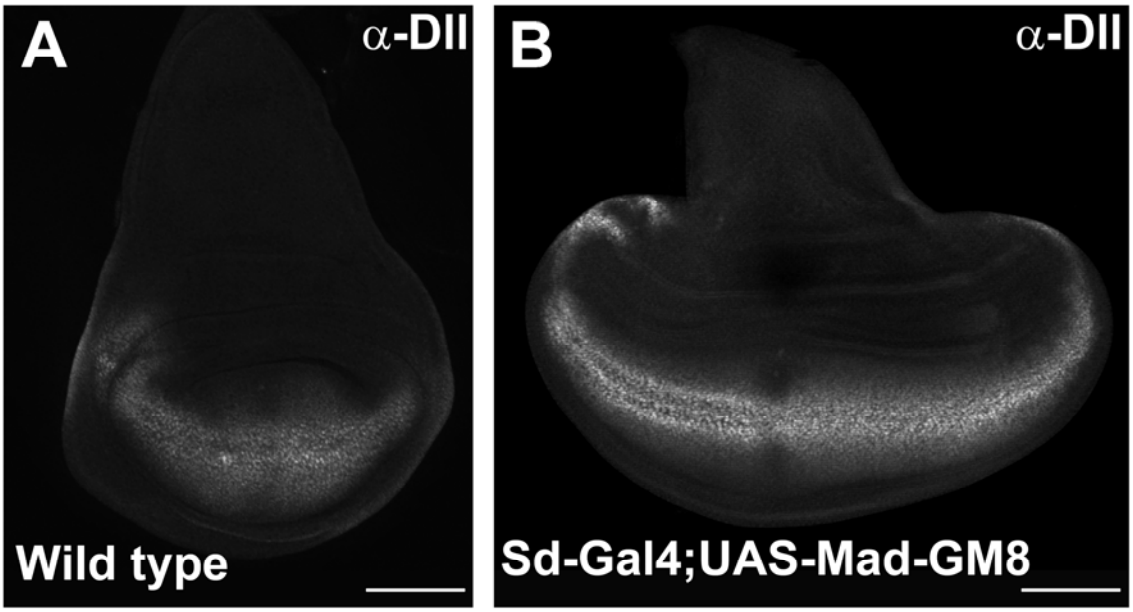

figure S2. Mad-GM8 expression increases the area of Distalless, a downstream target of Wg. **(A)** Distribution of Distalless in a wild-type wing imaginal disc at 3rd instar larval stage (n = 24 discs). Distalless is strongest along the presumptive wing margin and weaker in other regions of the wing pouch (n = 14 discs). **(B)** Overexpression of Mad-GM8 using Scalloped-Gal4 wing disc increases the area of Distalless in the wing pouch (n = 15). The shape of the wing disc is also extended along the anterior-posterior axis, and the overall size increased, as is typical of wing discs with increased Dpp signaling (*3*). Scale bars, 100 μm.

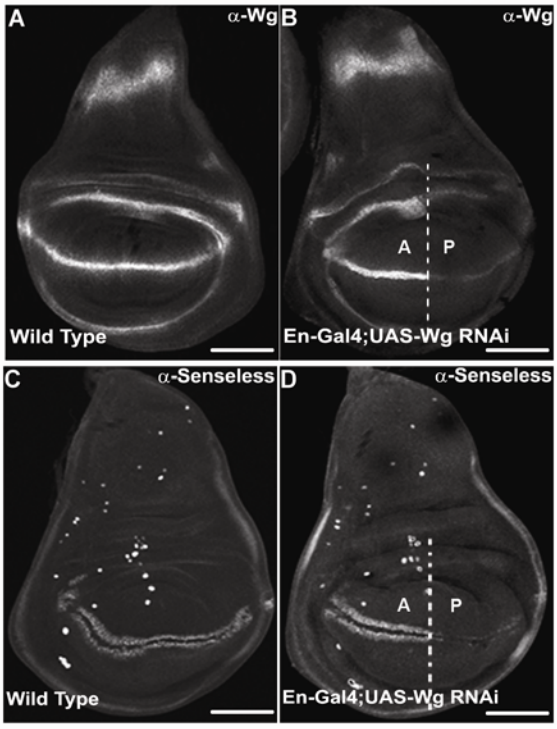

figure S3. Inducible RNAi directed against Wg depletes Wg protein and its downstream target Senseless. **(A)** Wild-type distribution of Wg protein in 3rd instar larval wings imaginal discs (n = 20 discs). **(B)** Wg RNAi in the posterior (P) wing compartment driven by *Engrailed-Gal4* reduced Wg protein abundance (n = 18). **(C)** Wild-type distribution of Senseless, a downstream target of Wg target (n = 40 discs). **(D)** Senseless is lost in the posterior wing compartment when Wg is knocked down by RNAi driven by *Engrailed*-Gal4 (n = 23 discs). These results demonstrate that the Wg RNAi construct used (VDRC #13352) is effective in *Drosophila*. Scale bars, 100 μm.

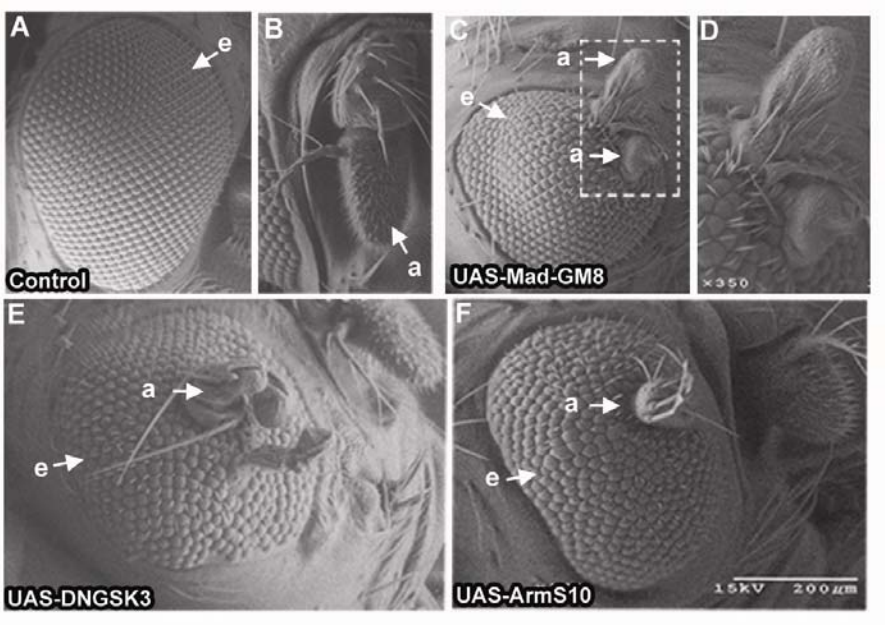

figure S4. Mad-GM8 expression in the eye imaginal disc produces phenotypes suggestive of high Wg signaling. **(A)** Image of wild-type adult eye (e) and **(B)** antenna (a) by scanning electron microscopy. **(C)** Transformation of part of the *Drosophila* eye into antennal-like tissue when Mad-GM8 was driven by *eyeless-Gal4* (n = 66 eyes with ectopic antennae or bulging structures out of 97 eyes). **(D)** A high power image of two ectopic antennal-like growths induced by Mad-GM8 overexpression. **(E)** Similar antennal-like structures were observed when Wg signaling was activated by dominant negative GSK3 (DNGSK3) (n = 24 eyes) or **(F)** stabilized Armadillo (ArmS10) driven by *eyeless-Gal4* (n = 13 eyes). This experiment shows that overexpression of the stabilized, GSK3 phosphorylation-resistant form of Mad elicits a canonical Wg signal.

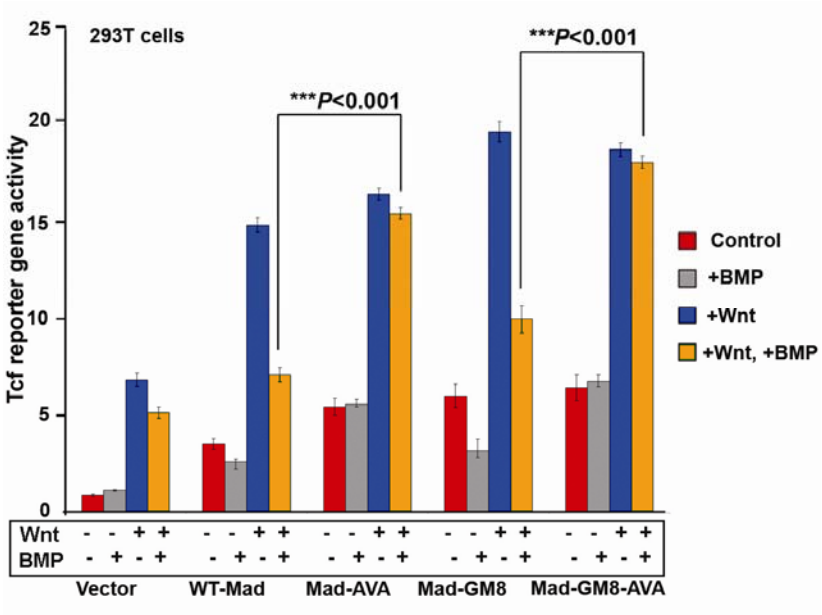

figure S5. C-terminal phosphorylation of Mad enables BMP4 to repress the Mad-induced increase in Tcf reporter gene activity. Mad forms resistant to phosphorylation by BMP receptor are insensitive to inhibition of Wnt signaling by BMP4. W-Mad or Mad mutant proteins (Mad-AVA, Mad-GM8, or Mad-GM8-AVA) increased Wnt reporter activity compared to control cells. A comparable increase in Wnt activity was found when cells were transfected with WT-Mad or Mad-AVA (the C-terminal phosphorylation mutant), an effect that can be attributed to the lack of endogenous BMP signaling in HEK293T cells. In the case of *Drosophila* S2R+ cells, which have endogenous BMP signaling, Mad-AVA stimulated the activity Tcf reporter (Fig. 2B). Expression of a form of Mad with mutations in the 8 putative GSK3 phosphorylation sites in the linker region increased Wnt reporter activity compared to WT-Mad. Also, BMP4 treatment of cells failed to induce significant Tcf reporter activation (grey bars). Treating cells with both Wnt and BMP4 inhibited the ability of WT-Mad to increase Wnt-reporter activity, but not in cells expressing C-terminal mutant forms of Mad (Mad-AVA and Mad-GM8-AVA; see brackets). We propose that phosphorylation of Mad by BMP receptor prevents Mad from signaling in the Wnt pathway (n = 3 experiments; statistical analysis was carried out with a 2-way ANOVA with

Tukey's post-test).

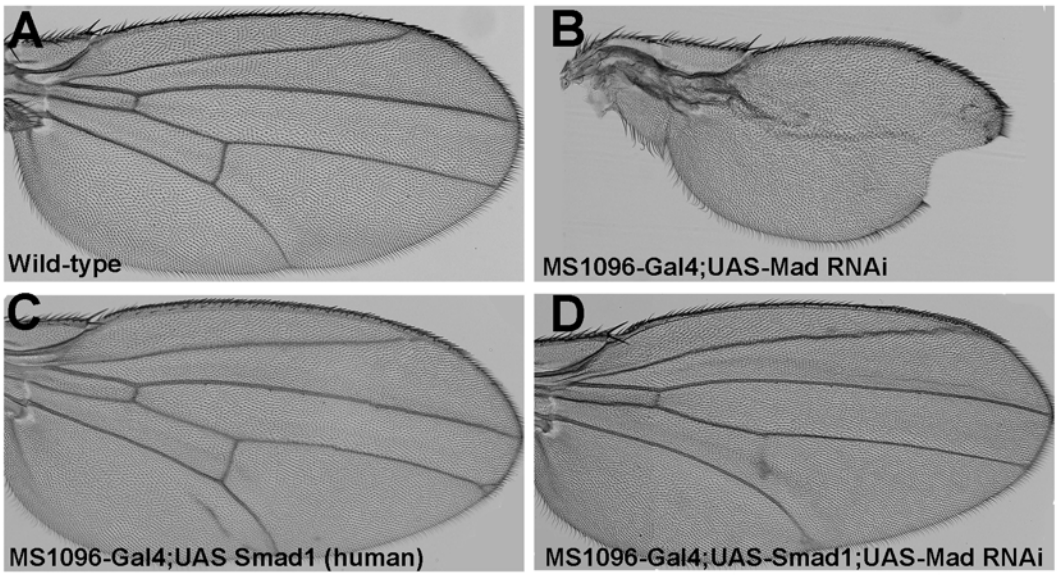

figure S6. The Mad RNAi phenotype is rescued by coexpression of a human Smad1 transgene. **(A)** Wild-type adult wing, showing normal venation, which requires BMP signaling (n = 30 wings). **(B)** Loss of vein tissue and margin notching in Mad-RNAi adult wings (n = 25). **(C)** Overexpression of a UAS-Smad1 human produced some extra vein tissue, but the wing was largely normal (n=15). **(D)** The Mad RNAi phenotype was rescued (except for the posterior crossvein) when a human Smad1 transgene was expressed (n=9).

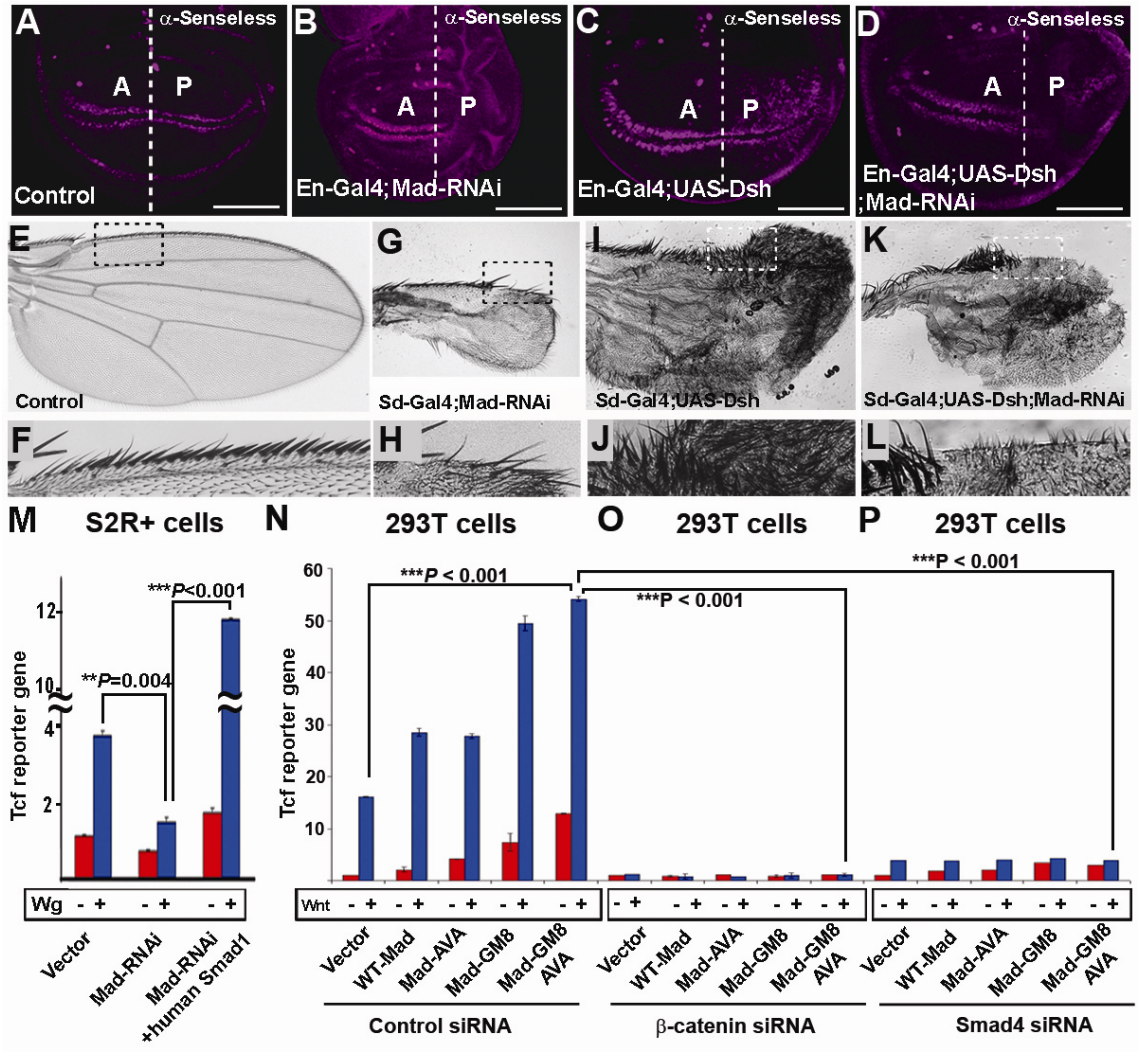

figure S7. Mad is required for Wg signal transduction during wing margin development. **(A)** Distribution of Senseless in 3rd instar wild-type wing imaginal disc. Anterior-posterior axis of the wing disc is indicated as A and P. **(B)** Mad knockdown using an RNAi driven by Engrailed-Gal4 specifically in the posterior wing compartment reduces the area of Senseless. **(C)** Overexpression of Dishevelled in the posterior compartment causes ectopic areas of Senseless. **(D)** Ectopic Senseless is blocked by Mad-RNAi expression in the posterior compartment. Mad RNAi is epistatic to Dishevelled, indicating that Mad is required downstream of Dishevelled in the Wnt pathway. At least 12 imaginal discs were analyzed for each genotype, all with similar

phenotypes. **(E)** Wild-type adult wing. **(F)** High magnification of the anterior wing margin (highlighted as a boxed region in E). **(G** and **H)** Mad RNAi driven with Scalloped-Gal4 results in a small veinless wing. This wing is deficient in margin bristles, which suggests loss of Wg signaling (n = 45 wings). **(I** and **J)** Overexpression of Dishevelled caused increased bristle formation throughout the wing blade (n = 38 wings). **(K** and **L)** Increased bristle formation in the wing blade caused by Dishevelled was inhibited when Mad was knocked down using RNAi (n = 24). **(M)** Mad knockdown by Gal4-inducible RNAi inhibited Tcf reporter gene activation, which was rescued by transfection of human WT-Smad (n = 5 experiments, statistical analysis carried out using a 2-way ANOVA with Tukey's post-test). **(N** to **P)** Activation of the Tcf reporter gene by Mad constructs in the presence of control siRNA, β-catenin siRNA, or Smad4 siRNA in HEK293T cells. Treating cells with a control siRNA had no effect on Tcf reporter gene activation. siRNA-mediated depletion of β-catenin blocked activation of the canonical Wnt pathway. Treatment of cells with Smad4 siRNA also efficiently blocked Wnt signaling. This shows that both Smad4 and β-catenin are essential components of the Wnt signaling pathway (n = 3 experiments, statistical analysis carried out using a 2-way ANOVA with Tukey's post-test). Scale bars 100 μm.

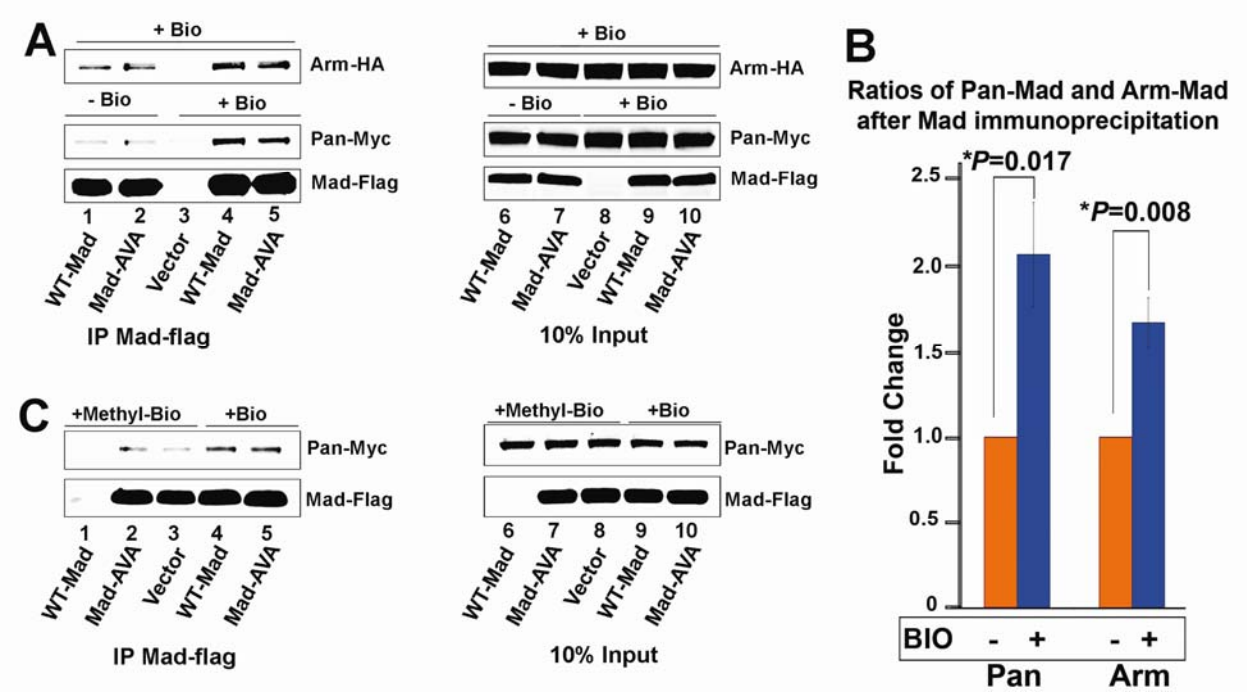

figure S8. Inhibition of GSK3 activity by BIO enhances the binding of Mad to Pangolin. **(A)** Coimmunoprecipitation of Pangolin-Myc and Armadillo-HA through Mad-Flag or Mad-AVA-Flag (lanes 1-5). Pangolin and Mad DNAs were transfected separately into HEK293T cells and treated with or without the GSK3 inhibitor BIO. Cells expressing Armadillo were subjected to BIO treatment under all conditions to ensure sufficient protein amounts. Input proteins (lanes 6-10) shown are 10% of the amount used for the binding experiments. Cell lysates containing Mad proteins were incubated with separate lysates containing Pangolin and Armadillo proteins for one hour at 4^{o}C to allow binding. In the absence of BIO, we observed only weak binding between Mad and Pangolin (lanes 1 and 2, minus BIO). Treating HEK293T transfected cells with BIO enhanced the binding of Mad to Pangolin (lanes 4 and 5, +BIO), indicating that the phosphorylation of Mad by GSK3 inhibits binding between Mad and Pangolin. Based on these findings, we propose that Wnt signaling promotes the binding of Mad to Pangolin by preventing GSK3 phosphorylations, in addition to stabilizing Armadillo (n = 3 experiments). **(B)** Quantification of the ratio of immunoprecipitated Pangolin and Armadillo protein over Mad

using a LI-COR Odyssey scanner system. Treatment with the GSK3 inhibitor BIO caused a 2-fold increase in binding efficiency between Mad and Pangolin and a 1.5 -fold increase in binding efficiency to Armadillo in HEK293T cell extracts (P = 0.0017, P = 0.008, Mann-Whitney Wilcoxon test, n = 3). **(C)** We also used an inactive form of this compound, methylated-BIO, to test whether BIO had non-specific off target effects. In cells treated with methylated-BIO, there was less binding of Mad to Pangolin (lanes 2 and 3) when compared to the active form of BIO (lanes 4 and 5).

Table S1. Primer Sequences: Primers used for the double stranded RNAi experiments and the Biotin labeled primers used to PCR the 7x TOPFLASH or FOPFLASH Pangolin binding sites for DNA Affinity Precipitation Assay (DAPA)

Primer name	Sequence
dsRNA Mad 5’	TTAATACGACTCACTATAGGGAGAGTCATGGTCACACTGTTTTCAATGG
dsRNA Mad 3’	TTAATACGACTCACTATAGGGAGACTGTTGCTGCTGCCGCTGATTGCTG
dsRNA Med 5’	TTAATACGACTCACTATAGGGAAGTGCGTGACCATACAGCGCACC
dsRNA Med 3’	TTAATACGACTCACTATAGGGATTCAGAGGGACCCTGTGGATATCCG
dsRNA Arm 5’	GGATTAATACGACTCACTATAGGGAGACAACTGAGCCAGACACGC
dsRNA Arm 3’	GGATTAATACGACTCACTATAGGGAGAGCTCTCCTGGTTACCATAGG
DAPA primer 5’	Biotin-CAGGTGCCAGAACATTTCTC
DAPA primer 3’	AAGCTGGAATTCGAGCTTCC

References

1. E. Eivers, L.C. Fuentealba, V. Sander, J.C. Clemens, L. Hartnett, E.M. DeRobertis, Mad is required for Wingless signaling and segment patterning in Drosophila and Xenopus. *PLoS One* **4**, e6543 (2009).
2. J. P. Couso, S. A. Bishop, A. Martinez-Arias, The wingless signalling pathway and the patterning of the wing margin in Drosophila. *Development* **120**, 621-636 (1994).
3. T. Lecuit, W.J. Brook, M. Ng, M. Calleja, H. Sun, S.M. Cohen. Two distinct mechanisms for long-range patterning by Decapentaplegic in the Drosophila wing. *Nature* **381**, 387-393 (1996).